The exocyst subunit *CsExo70B* promotes both fruit length and disease resistance via regulating receptor kinase abundance at plasma membrane in cucumber

Liu Liu[1], Jiacai Chen[1], Chaoheng Gu[1], Shaoyun Wang[1], Yufan Xue[1], Zhongyi Wang[1], Lijie Han[1], Weiyuan Song[1], Xiaofeng Liu[1], Jiahao Zhang[1], Min Li[1], Chuang Li[1,2], Liming Wang[1], Xiaolan Zhang[1,2,]* (iD) and Zhaoyang Zhou[1,2,]* (iD)

[1]*State Key Laboratories of Agrobiotechnology, Joint International Research Laboratory of Crop Molecular Breeding, Beijing Key Laboratory of Growth and Developmental Regulation for Protected Vegetable Crops, Department of Vegetable Sciences, China Agricultural University, Beijing, China*
[2]*Sanya Institute of China Agricultural University, Sanya, China*

Summary

Plant defence against pathogens generally occurs at the expense of growth and yield. Uncoupling the inverse relationship between growth and defence is of great importance for crop breeding, while the underlying genes and regulatory mechanisms remain largely elusive. The exocytosis complex was shown to play an important role in the trafficking of receptor kinases (RKs) to the plasma membrane (PM). Here, we found a *Cucumis sativus* exocytosis subunit Exo70B (CsExo70B) regulates the abundance of both development and defence RKs at the PM to promote fruit elongation and disease resistance in cucumber. Knockout of *CsExo70B* resulted in shorter fruit and susceptibility to pathogens. Mechanistically, CsExo70B associates with the developmental RK CsERECTA, which promotes fruit longitudinal growth in cucumber, and contributes to its accumulation at the PM. On the other side, CsExo70B confers to the spectrum resistance to pathogens in cucumber via a similar regulatory module of defence RKs. Moreover, *CsExo70B* overexpression lines showed an increased fruit yield as well as disease resistance. Collectively, our work reveals a regulatory mechanism that CsExo70B promotes both fruit elongation and disease resistance by maintaining appropriate RK levels at the PM and thus provides a possible strategy for superior cucumber breeding with high yield and robust pathogen resistance.

Introduction

In nature, plants constantly encounter a variety of pathogens, and they have evolved sophisticated defence mechanisms to against pathogens. However, prolonged defence often leads to growth inhibition and yield penalty (Huot *et al.*, 2014). On the other hand, the rapid growth of plants is usually accompanied by increased susceptibility to pathogens (He *et al.*, 2022). One prevailing explanation for this phenomenon is energy competition, in which the limited resource drives the trade-off between growth and defence (Coley *et al.*, 1985; Herms and Mattson, 1992). Despite recent studies showed that genetic manipulation of single proteins, such as transcription factors (TFs) and aquaporins (AQPs), or of different genes simultaneously can make plants grow well and defend better (He *et al.*, 2022; Lu *et al.*, 2022; Wang *et al.*, 2018; Xu *et al.*, 2022), the underlying genes and regulatory mechanisms of growth-defence balance remain largely elusive.

Receptor-like kinases (RLKs) are encoded by expanded gene families and can act as receptors, co-receptors, and regulatory partners. They play vital roles in plant growth, development, and adaptation to diverse environmental conditions (Liang and Zhou, 2018; Morris and Walker, 2003; Shiu and Bleecker, 2001a,b). Many RLKs function as immune receptor kinases (RKs) to sense conserved molecular patterns derived from microbes or plants during potential pathogen infection to activate

plant defence (Couto and Zipfel, 2016; Gust *et al.*, 2017). For example, the FLAGELLIN SENSING 2 (FLS2) and ELONGATION FACTOR-TU (EF-Tu) RECEPTOR (EFR) are the receptors of a conserved 22 amino acid epitope (flg22) and elf18 derived from bacterial flagellin and elongation factor, respectively (Gómez and Boller, 2000; Zipfel *et al.*, 2004, 2006). Similarly, LysM-RKs LYSINE MOTIF RECEPTOR KINASE5 (LYK5) senses fungal chitin and activates downstream immune responses (Cao *et al.*, 2014). Other RKs have been shown to recognize endogenous peptides to regulate plant development. For example, two different RKs including CLAVATA1 (CLV1) and RECEPTOR-LIKE PROTEIN KINASE 2 (RPK2) perceive the secreted peptide CLAVATA3 (CLV3) to limit shoot apical meristem size (Clark *et al.*, 1997; Kinoshita *et al.*, 2010). A disulphated pentapeptide phytosulfokine (PSK) plays a ubiquitous role in plant growth and development (Matsubayashi, 2014), which perceived by the receptor PSKR in carrot and *Arabidopsis* (Amano *et al.*, 2007; Matsubayashi *et al.*, 2002). Moreover, ERECTA (ER) senses the secreted cysteine-rich peptides of EPF/EPFL family to regulate many biological processes including longitudinal growth of aboveground organs and reproductive development (Shpak, 2013; Shpak *et al.*, 2003). The appropriate abundance of RKs at plasma membrane (PM) is critical for signal recognition and transduction. Nonetheless, only a few of regulators that function in the trafficking of RKs were identified in plants. For instance, the ER-resident proteins RETICULAN LIKE PROTEIN B1/2 (RTNLB1/2) and

RABA1b regulate the trafficking of de novo-synthesized FLS2 out of the endoplasmic reticulum and *trans*-Golgi network (TGN) to the PM, respectively (Choi *et al.*, 2013; Lee *et al.*, 2011).

Recently, exocyst complex has been shown to play an important role in maintenance of the abundance of cargos at PM (Saeed *et al.*, 2019). The exocyst was initially identified in yeast and contains eight protein subunits: Sec3, Sec5, Sec6, Sec8, Sec10, Sec15, Exo70 and Exo84. It mediates the tethering process of secretory vesicles to the PM (TerBush *et al.*, 1996). In particular, Sec3 and Exo70 work as vital tethers that guarantees the first contact between vesicles and PM, followed by the soluble N-ethylmaleimide-sensitive factor attachment protein receptor (SNARE) mediates membrane-fusion (Saeed *et al.*, 2019). In plants, Exo70 has the most copies and is broadly involved in multiple biological processes (Chong *et al.*, 2010; Zárský *et al.*, 2009). In *Arabidopsis*, Exo70A1 has been reported to be involved in the secretion of PIN-FORMED (PIN) transporters to the PM and polar auxin transport and then regulates the apical dominance and organ morphogenesis (Drdová *et al.*, 2013; Synek *et al.*, 2006). Exo70H4 mediates the secretion of a stress-induced callose synthase powdery mildew resistant 4 (PMR4) to PM and functions in the development of inner cell wall layer (Kulich *et al.*, 2015, 2018). Beyond that, Exo70B1 and Exo70B2 are the vital regulators of pattern-triggered immunity (PTI) response, *exo70b1–3* and *exo70b2* mutants both displayed more suscep-tibility to *Pseudomonas syringae* pv. *tomato* (*Pto*) strain DC3000 (Stegmann *et al.*, 2012, 2013). A recent study showed that Exo70B1 and Exo70B2 function in trafficking FLS2 to the PM, possibly by tethering the FLS2-containing vesicles to the targeted PM, thereby regulating plant defence response in *Arabidopsis* (Wang *et al.*, 2020a). Similarly, OsExo70B1 interacts with the RK-chitin elicitor receptor kinase 1 (CERK1), the co-receptor of chitin, to resist the *Magnaporthe oryzae* (*M. oryzae*) in rice (Hou *et al.*, 2020). Above these suggested that Exo70B mainly regulates plant resistance via trafficking the RKs to the PM. However, whether Exo70B regulates developmental RKs in a similar mode remains largely unknown.

Cucumber (*Cucumis sativus* L.) is an economically important vegetable crop, which bears pepo fruits harvested immaturely at 8–18 days after anthesis (DAA) (Pan *et al.*, 2017; Che *et al.*, 2023), but its production is substantially affected by various diseases (Weng and Wehner, 2017). The most important pathogens that affect cucumber include the *Fusarium oxysporum* f. sp. *Cucumerinum Owen* (*Foc*) and *Pseudomonas syringae* pv. *lachrymans* (*Psl*), which cause fusarium wilt (also known as cancer) and angular leaf spot in cucumber, respectively (Chand and Walker, 1964; Dong *et al.*, 2019). In this study, we showed a *CsExo70B* positively regulates both fruit elongation and disease resistance. Further analyses revealed that CsExo70B associates with multiple RKs, including CsERECTA, CsFLS2 and CsLYK5 and promotes their accumulation at the PM. More importantly, overexpression of *CsExo70B* resulted in an increase of cucumber fruit yield and disease resistance. Together, our findings provide a strategy to enhance cucumber yield and resistance.

Results

CsExo70B positively regulates fruit elongation in cucumber

Previous studies showed that Exo70B members are involved in immunity by regulating the accumulation of RK-FLS2 at PM in *Arabidopsis* (Wang *et al.*, 2020a). To explore whether Exo70B regulates plant development by associating with RKs, we identified the Exo70B in cucumber (*CsaV3_1G036490*) and named as *CsExo70B* hereafter (Liu *et al.*, 2023). CRISPR/Cas9 method was used to generate *Csexo70b* knockout mutants. Two homozygous mutants were obtained. The *Csexo70b-5#* allele has 29 bp deletion and 3 bp replacement, and *Csexo70b-4#* allele has 131 bp deletion. Both mutations resulted in premature stop codon at 136[Arg] and 156[Tyr], respectively (Figure 1a, Figure S1a). There were no off-target loci detected in both mutants (Table S1). Interestingly, we found that the fruit length was significantly reduced in *Csexo70b* lines at all observed stages including anthesis, 10 DAA, and 30 DAA (Figure 1b–d). The fruit length of *Csexo70b-5#* and *Csexo70b-4#* mutants have a 21.9% and 29.45% reduction at anthesis, 36.37% and 35.3% reduction at 10 DAA, and 25.6% and 26.8% reduction at 30 DAA compared to that of wild type (WT) plants in the corresponding periods (Figure 1e–g). Moreover, the microscopic structures of longitudinal sections of the fruit pericarp at 10 DAA were examined for WT and *Csexo70b* mutants. We found that the cell size of *Csexo70b* mutants was 15.2% smaller, and the cell number was also reduced 19.4% compared to that in WT plants. These results suggested that CsExo70B promotes fruit elongation by stimulating both cell expansion and cell division (Figure 1h–k). Furthermore, the *Csexo70b* mutants also displayed slightly dwarfed plant height, smaller male flowers and seeds, as well as increased carpels in cucumber (Figure S1b–h), indicating that *CsExo70B* plays an important role in cucumber development.

CsExo70B directly interacts with CsERECTA and affects its accumulation at PM

Considering the roles of CsExo70B in multiple aspects of development, we explored whether CsExo70B interacts with some development-related RKs using firefly split-luciferase complementation (luc) assay (Figure S2). Very interestingly, we found CsExo70B strongly associated with CsERECTA (Figure S2), a founding RK regulating silique length in *Arabidopsis* (Pillitteri *et al.*, 2007; Shpak *et al.*, 2003). To investigate the function of *CsERECTA* in cucumber, we also used CRISPR/Cas9 system to knock out *CsERECTA*. Two mutant alleles *Cserecta-2#* (with 1 bp insertion and 4 bp deletion) and *Cserecta-12#* (with 1 bp and 3 bp deletions) were obtained. Both mutations resulted in premature stop, generating truncated proteins of 31 amino acids and 39 amino acids, respectively (Figure 2a, Figure S3a), and no off-target loci were detected (Table S1). As expected, *Cserecta* mutants exhibited significantly shorter fruits from anthesis to 30 DAA (Figure 2b–d). The average fruit length of *Cserecta-2#* and *Cserecta-12#* mutants had a 40.8% and 36.15% reduction at anthesis, 51.28% and 51.94% reduction at 10 DAA, and both 40% reduction at 30 DAA compared to that in WT (Figure 2e–g). Further study showed that cell size and cell number was significantly decreased in *Cserecta* mutants (Figure 2h–k), suggesting that CsERECTA also positively regulates fruit length by promoting cell expansion and cell division. In addition, *Cserecta* mutants also resulted in similar phenotypes to *Csexo70b* mutants, including dwarfed plants, and reduced size of male flowers and seeds (Figure S3b–i).

The same phenotypes of *Csexo70b* and *Cserecta* promoted us to test if CsExo70B regulates CsERECTA accumulation at PM. First, we sought to verify that CsExo70B interacts with CsERECTA
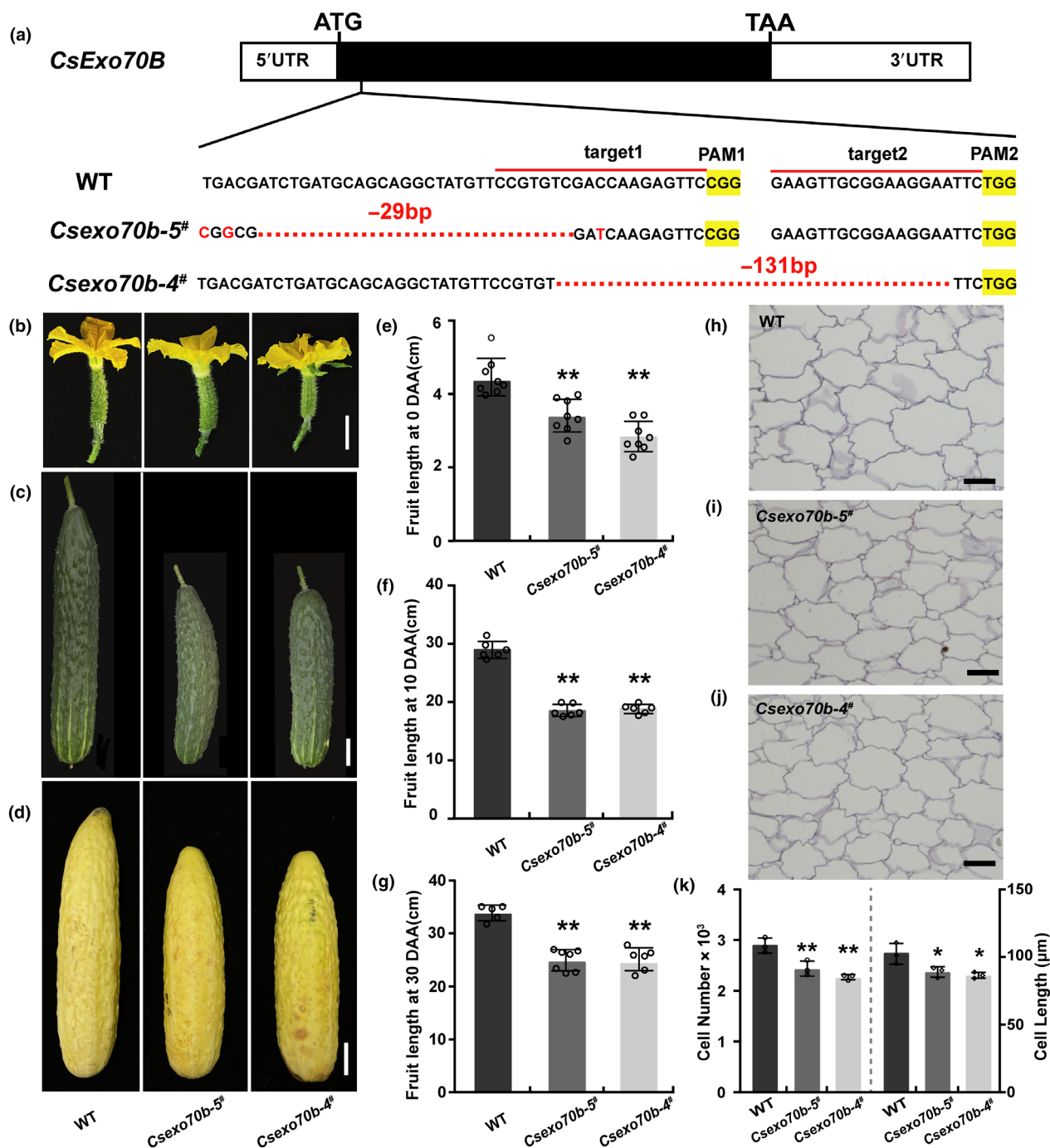
Figure 1 Construction and characterization of the *Csexo70b* mutants in cucumber. (a) CRISPR/Cas9-mediated mutations of *CsExo70B* gene. The single-guide RNAs (sgRNAs) are marked in red line, and protospacer-adjacent motif (PAM) sites are highlighted in yellow. '−29' and '−131'-bp indicate frame shifts in *Csexo70b* mutant lines. (b–d) Morphology of ovaries at anthesis (b), fruits at 10 days after anthesis (DAA) (c), and 30 DAA (d) in wild type (WT) and *Csexo70b* mutants, scale bar = 1 cm (b) or 3.5 cm (c, d). (e–g) Statistical analyses of ovary length shown in (b) and fruit length observed in (c) and (d). Values are means ± SD, $n \geq 5$. (h–j) Longitudinal pericarp sections of fruits at 10 DAA in WT and *Csexo70b* mutants, scale bar = 100 μm. (k) The cell number and cell length quantification of fruit pericarp in WT and *Csexo70b* mutants along a longitudinal axis. Values are means ± SD, n = three individual fruits. Significant differences relative to WT are indicated by asterisks (*$P < 0.05$; and **$P < 0.01$, one-way ANOVA).

using multiple assays. As shown in Figure 3a and Figure S4, the split-luc and the bimolecular fluorescence complementation (BiFC) assays in *Nicotiana benthamiana* (*N. benthamiana*) indicated that CsExo70B interacted with CsERECTA, but not CsBAK1.

The CsExo70B-CsERECTA interaction was also detected using co-immunoprecipitation (co-IP) assays when a FLAG-tagged CsERECTA was co-expressed with CsExo70B-HA in *N. benthaminana* (Figure 3b). Co-IP experiments using stable
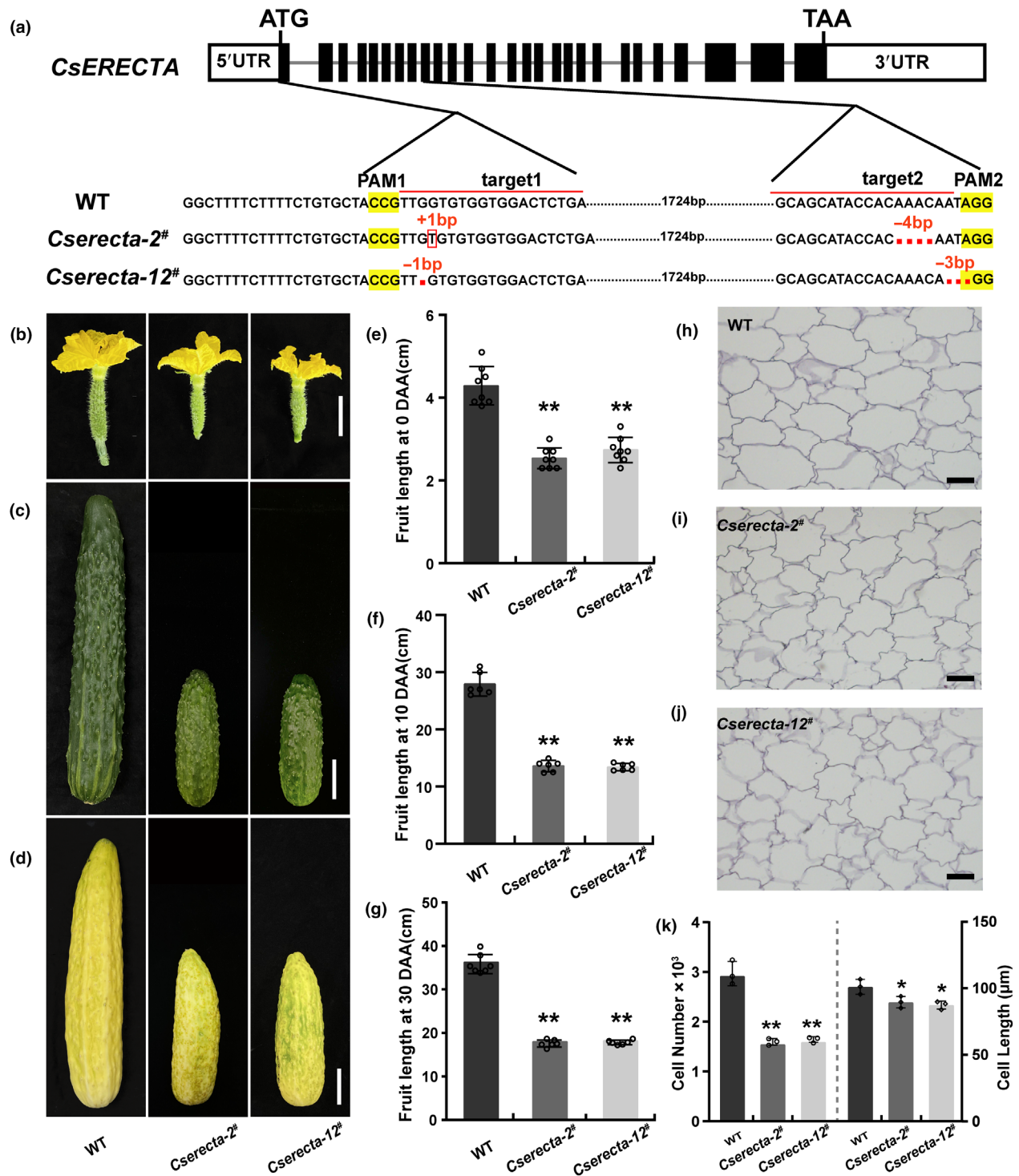
Figure 2 Phenotypic characterization of *CsERECTA* knockout lines in cucumber. (a) Mutant alleles of *Cserecta*. The red-lined sequences in the WT denote the regions targeted by sgRNA. The *Cserecta-2#* allele has 1-bp insertion and 4-bp deletion, and the *Cserecta-12#* allele has 1-bp and 3-bp deletions. (b–d) The fruit morphology of WT and *Cserecta* mutants. Pictures were collected at anthesis (b), 10 DAA (c) and 30 DAA (d). Scale bar = 2 cm in (b), 3.5 cm in (c), and 5 cm in (d). (e–g) The length quantification of fruits in (b–d). Data are shown as means ± SD; $n \geq 6$. Significant differences relative to WT are indicated by asterisks (**$P < 0.01$, one-way ANOVA). (h–j) Longitudinal sections of fruit pericarp at 10 DAA of WT and *Cserecta* mutants. Scale bar = 100 μm. (k) Statistical analyses of cell number and cell length phenotypes along a longitudinal axis. Data are shown as means ± SD; n = three individual fruits. Statistical significances were determined by one-way ANOVA (*$P < 0.05$; **$P < 0.01$).

CsExo70B-HA transgenic plant roots which expressing with CsERECTA-FLAG further confirmed the CsExo70B-CsERECTA interaction in cucumber plants (Figure 3c).

To further investigate if CsExo70B regulates protein accumulation of CsERECTA at the PM, we developed peptide-specific antibodies recognizing CsERECTA and CsH+-ATPase. The

specificity of CsERECTA antibody was confirmed by Western blot using the lysates from WT and *Cserecta* mutants and *N. benthamiana* leaves (Figure S5a,b), CsH⁺-ATPase antibody

specificity was also confirmed in cucumber (Figure S5c). Total proteins were extracted from ovaries and PM fractions were separated, followed by CsERECTA detection with specific
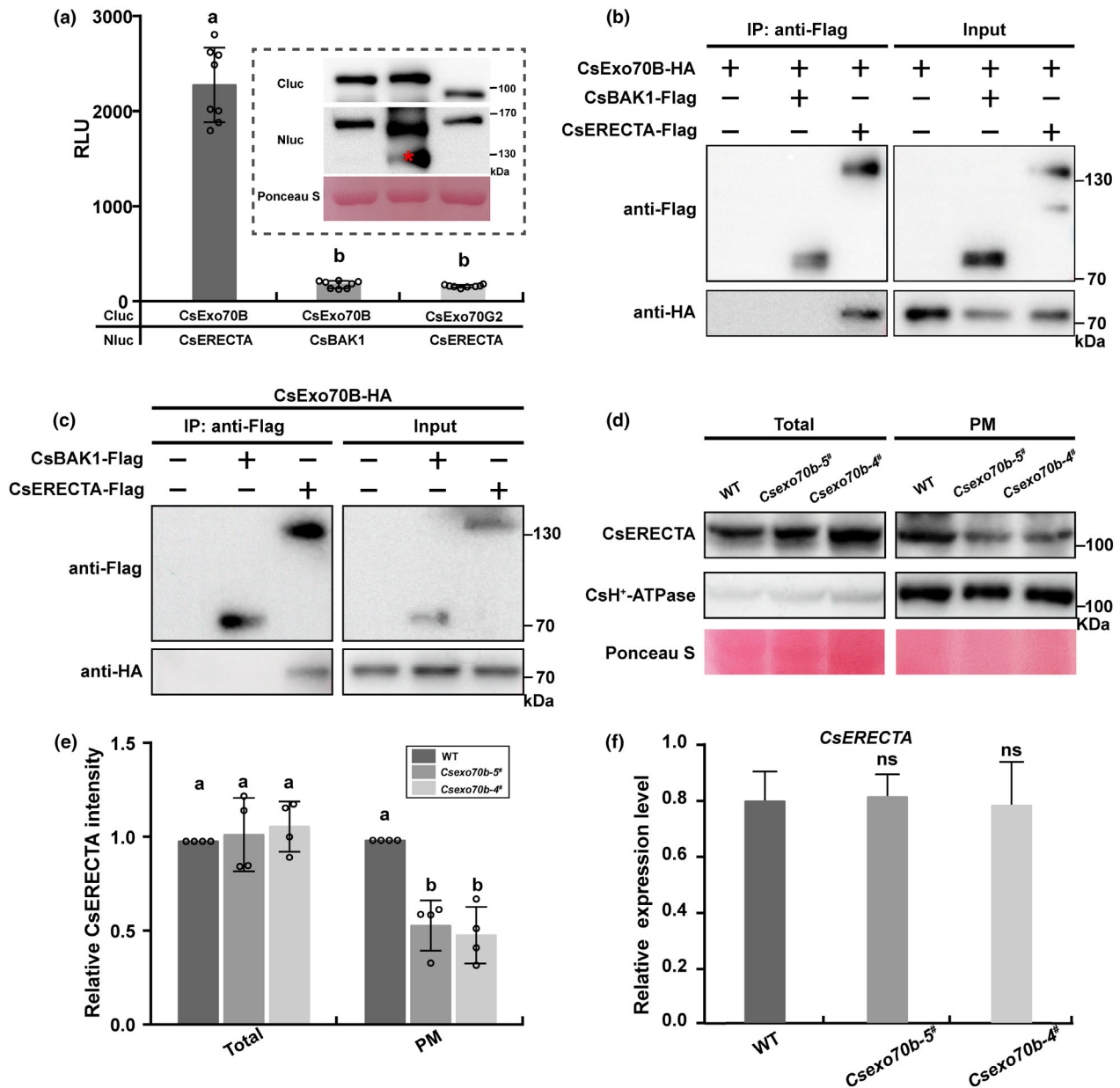

Figure 3 CsExo70B interacts with CsERECTA and contributes to its accumulation at plasma membrane (PM). (a) Firefly split-luciferase complementation (LUC) assay showed CsExo70B interacts with CsERECTA. The indicated constructs were expressed in *Nicotiana benthamiana* (*N. benthamiana*) leaves, and the relative LUC activity was recorded by a luminometer. Immunoblot showing the Cluc and Nluc fusion proteins, as determined by anti-Cluc and anti-HA antibodies, respectively. RLU, relative luminescence unit. Data are represented as means $\pm$ SD, $n = 8$. Different lowercase letters indicated statistically significant differences ($P < 0.01$, one-way ANOVA analysis with Tukey's test). (b) Co-immunoprecipitation (IP) of CsExo70B and CsERECTA in *N. benthamiana* leaves. These indicated constructs were expressed in *N. benthamiana* leaves, and co-IP assay was performed by anti-FLAG antibody. CsBAK1-FLAG was used as a negative control. (c) Co-IP assay between CsExo70B and CsERECTA in cucumber roots. The CsERECTA-FLAG was expressed in hairy roots of stable *CsExo70B-HA* overexpression lines using *Agrobacterium rhizogenes* mediated transformation, and co-IP assay was performed by anti-FLAG antibody. (d) Immunoblotting analysis of endogenous CsERECTA levels in different fractions. CsH⁺-ATPase was used as PM protein marker. Total and PM proteins were extracted from ovaries and detected by anti-CsERECTA antibody. Equal loading was demonstrated by Ponceau Staining (Ponceau S) of Rubisco. (e) Statistical analysis of the relative CsERECTA levels from four independent replicates. Numbers indicate relative protein band density of CsERECTA normalized to CsH⁺-ATPase, and the data are means $\pm$ SD, $n = 4$. Different lowercase letters indicate statistically significant differences ($P < 0.05$, one-way ANOVA analysis with Tukey's test). (f) Transcript level of *CsERECTA* in WT and *Csexo70b* mutants. Data are means $\pm$ SD, $n = 3$ (ns, no significant difference, one-way ANOVA).
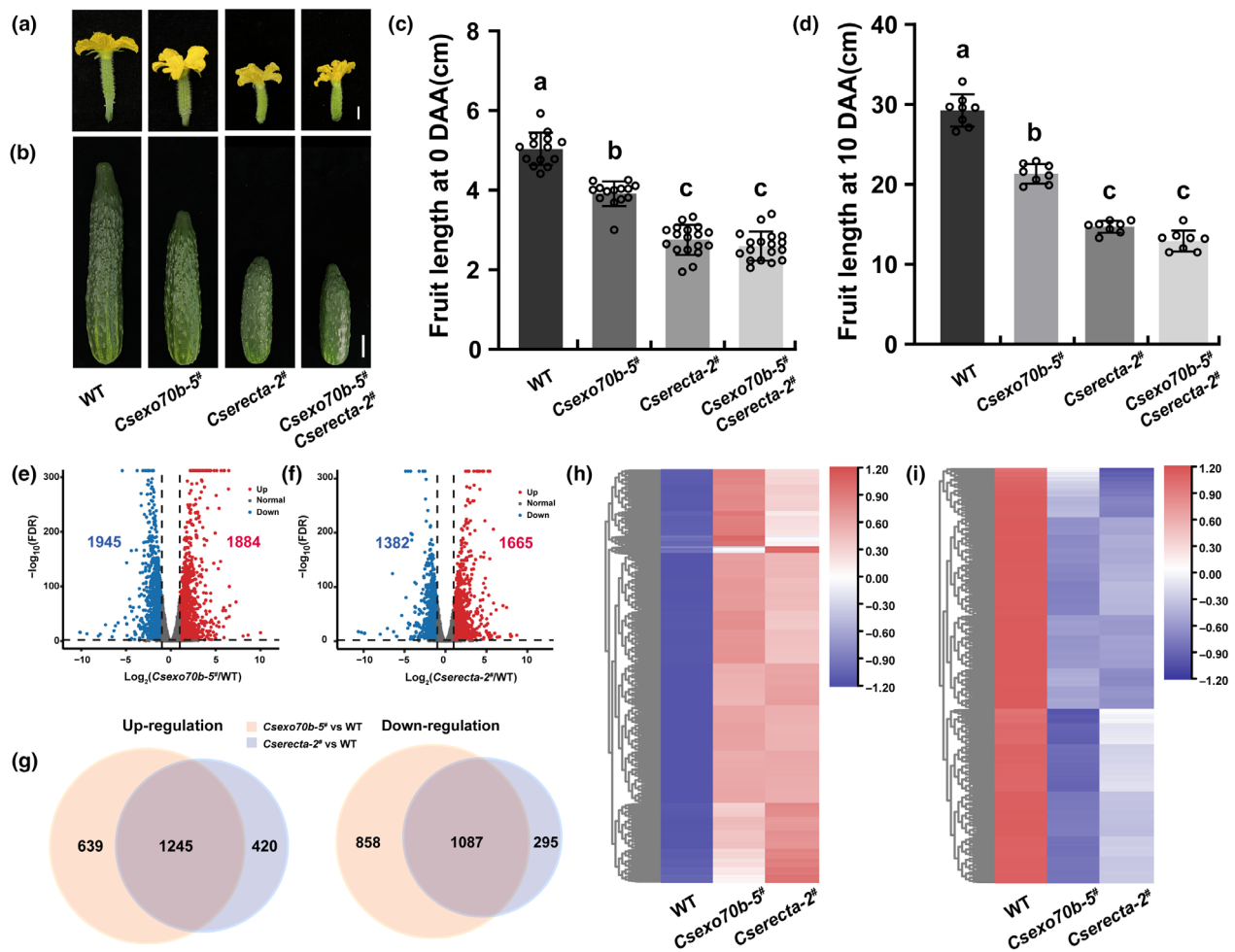
Figure 4 CsExo70B and CsERECTA co-regulate the fruit elongation in cucumber. (a, b) The morphology of fruit at anthesis (a) and 10 DAA (b) of WT, *Csexo70b-5*[#], *Cserecta-2*[#] and *Csexo70b-5*[#] *Cserecta-2*[#]. Scale bar = 1 cm in (a) and 3 cm in (b). (c, d) Quantification of fruit length in the indicated lines shown in (a) and (b). Values are means $\pm$ SD ($n \geq 7$). The different lowercase letters indicate significant differences ($P < 0.05$) by one-way ANOVA analysis with Turkey's test. (e, f) Transcriptome analysis for fruits at 3 DAA of WT, *Csexo70b-5*[#] and *Cserecta-2*[#] mutants. Volcano diagrams showing the differentially expressed genes (DEGs) in *Csexo70b-5*[#] (e) and *Cserecta-2*[#] (f) relative to WT (Fold change $\geq$ 2.0, FDR < 0.01). Down-regulated and up-regulated genes were appeared in bule and red, and grey means normal genes. (g) Veen diagrams showing the overlapped DEGs of *Csexo70b-5*[#] and *Cserecta-2*[#] mutants compared with WT, yellow and blue represent the DEGs in *Csexo70b-5*[#] and *Cserecta-2*[#] mutants, respectively. (h, i) Heat map showing the different expression patterns of shared DEGs in *Csexo70b-5*[#] and *Cserecta-2*[#] mutants. The data for each sample are averaged from three biological repeats.

antibody. In the *Csexo70b* mutants, less CsERECTA was detected in the PM fraction compared to WT, but there were no significant differences of total CsERECTA protein between *Csexo70b* mutants and WT (Figure 3d,e). Additionally, the transcripts of *CsERECTA* were not significantly different between WT and *Csexo70b* plants (Figure 3f), indicating that the reduced CsERECTA accumulation at PM in *Csexo70b* mutants is not a consequence of lower total levels. These results support the notion that CsExo70B specifically regulates the protein accumulation of CsERECTA at PM, thereby promoting fruit elongation in cucumber.

In addition, our results showed that CsExo70B also interacted with CsCLV1 in *N. benthamiana* (Figure S2). Consistent with the phenotype of *Csexo70b* mutants (Figure S1d,g), which has been reported that *CsCLV1* mutation leads to increased carpels in cucumber (Cheng *et al.*, 2022), we speculated that CsExo70B

may also regulate CsCLV1-mediated carpel development in cucumber. Together, these results demonstrate that CsExo70B associates with multiple RKs to regulate development in cucumber.

CsExo70B regulates fruit elongation through CsERECTA-mediated signal pathway in cucumber

To further confirm that CsExo70B and CsERECTA act in the same pathway to regulate fruit elongation in cucumber, we generated the *Csexo70b-5*[#] *Cserecta-2*[#] double mutant by crossing the *Csexo70b-5*[#] and *Cserecta-2*[#]. During the anthesis, the fruit length of *Csexo70b-5*[#] *Cserecta-2*[#] double mutants was indistinguishable from those of *Cserecta-2*[#] mutants, but significantly shorter than *Csexo70b-5*[#] mutants and WT lines (Figure 4a,c). The length of fruit at 10 DAA in *Csexo70b-5*[#] *Cserecta-2*[#] was slightly reduced, but still similar to that in *Cserecta-2*[#] (Figure 4b,d),

indicating that genetically *CsERECTA* acts downstream of *CsExo70B*.

In addition, we performed RNA-seq analyses for fruits of WT, *Csexo70b-5*[#], and *Cserecta-2*[#] plants. A total of 3829 differentially expressed genes (DEGs) were detected in *Csexo70b-5*[#] mutants and 3047 DEGs in *Cserecta-2*[#] mutants relative to WT (Fold change ≥ 2.0, FDR < 0.01) (Figure 4e,f). Among the 1665 up-regulated genes in *Cserecta-2*[#] mutants, 1245 genes were overlapped with DEGs in *Csexo70b-5*[#] mutants. Similarly, 1087 down-regulated genes in *Cserecta-2*[#] mutants were overlapped with DEGs in *Csexo70b-5*[#] mutants (Figure 4g), suggesting that the majority (76.5%) of transcripts were co-regulated by *CsExo70B* and *CsERECTA*. A heat map was generated to further show the expression patterns of these common DEGs in *Csexo70b-5*[#] and *Cserecta-2*[#] mutants (Figure 4h,i), which participated in multiple signalling pathways such as plant-pathogen interaction and plant hormone signal transduction (Figures S6 and S7, Tables S2 and S3). These data further support the notion that CsExo70B regulates fruit elongation through CsERECTA-mediated signal pathway in cucumber.

CsExo70B is required for resistance to fungal and bacterial pathogens

Previous studies showed that Exo70B members are required for plant immunity in *Arabidopsis* and rice (Hou *et al*., 2020; Wang *et al*., 2020a). Thus, we sought to dissect the disease resistance role of CsExo70B in cucumber. Firstly, we examined chitin- and flg22-induced ROS production in *Csexo70b* mutants. When treated with chitin, *Csexo70b* mutants accumulated 60%–70% less ROS compared with WT (Figure 5a). Similarly, flg22-induced ROS production was also reduced to 50%–60% in *Csexo70b* mutants compared with WT (Figure 5b).

To further confirm the function of *CsExo70B* in cucumber disease resistance, *Csexo70b* mutants and WT were firstly challenged with fungal vascular pathogen *Foc* using radicle dipping method (Figure S8a). We observed the severity of disease symptoms in both WT and *Csexo70b* mutants increased steadily with increasing days of infection. The disease symptom progression in *Csexo70b* mutants was earlier than that in WT plants. In *Csexo70b* mutants, minor disease symptoms firstly appeared at 7 days post-inoculation (dpi), severe wilting symptoms subsequently appeared in stem vascular and cotyledon at 10 dpi and 14 dpi, while in WT plants, only minor disease symptoms were observed until 10 dpi to 14 dpi (Figure S8b,c, Figure 5c). Consistently, the quantification of disease index (DI) and the percentage of disease grade in *Csexo70b* lines further confirmed this phenotype (Figure 5d, Figure S8d), indicating that the resistance to *Foc* in *Csexo70b* mutants is greatly reduced. Next, the *Csexo70b* and WT seedlings were spray-inoculated with bacterial leaf pathogen *Psl*. Three days after inoculation, more disease spots were observed in the *Csexo70b-5*[#] and *Csexo70b-4*[#] than WT, and the bacterial populations in the *Csexo70b-5*[#] and *Csexo70b-4*[#] mutants were approximately 2.6- to 3.6-fold greater than that in WT (Figure 5e,f). These results imply that *CsExo70B* positively regulates resistance to fungal and bacterial pathogens in cucumber.

CsExo70B associates with immune RKs and affects their abundance at the PM

The requirement of CsExo70B in RK signalling and resistance to bacterial and fungal pathogens promotes us to test whether CsExo70B similarly regulates immune RK abundance at the PM in cucumber. The well-known immune RKs FLS2 and LYK5, which perceive flg22 of bacterial flagellin and fungal chitin, respectively (Cao *et al*., 2014; Zipfel *et al*., 2004), were selected for further study. Multiple assays, including firefly Split-luc and BiFC assays in *N. benthamiana* leaves (Figure 6a,b, Figure S4), and Co-IP assays in *N. benthamiana* leaves (Figure 6c,d) and cucumber roots (Figure 6e,f), all showed that CsExo70B associated with CsLYK5 and CsFLS2 *in vivo*. To study if CsExo70B affects immune RK accumulation at PM in cucumber, we also developed peptide-specific antibodies recognizing CsLYK5 and CsFLS2. Unfortunately, only antibody of CsLYK5 was available (Figure S5d,e). Our results showed that CsLYK5 levels at PM in *Csexo70b-5*[#] and *Csexo70b-4*[#] were obviously reduced than that in WT, but the total protein and transcription levels of *CsLYK5* and *CsFLS2* were not changed in *Csexo70b* mutants (Figure 6g–i, Figure S9a), indicating that CsExo70B similarly affects immune RK accumulation at the PM, thus regulating disease resistance in cucumber.

Overexpression of *CsExo70B* enhances fruit yield and disease resistance in cucumber

The aforementioned results supported the notion that CsExo70B simultaneously maintains the abundance of developmental and immune RKs at the PM, regulating development and disease resistance in cucumber. To further test whether *CsExo70B* overexpression leads to higher yield and stronger defence, three stable overexpression transgenic lines were obtained. qRT-PCR results showed that the transcript levels of *CsExo70B* in *CsExo70B*-OE-3[#], *CsExo70B*-OE-4[#] and *CsExo70B*-OE-6[#] were 5.3-, 7.1- and 8.0-fold greater than WT. Immunoblot assay confirmed that CsExo70B-HA protein was accumulated in all *CsExo70B*-OE transgenic lines (Figure 7a). Compared to WT, *CsExo70B*-OE lines exhibited significantly longer fruits of both commercial and physiological maturity periods (Figure 7b,c, Figure S10a). We further explored fruit yield per plant in WT and *CsExo70B*-OE plants and observed 11.6%–22.9% higher yield in *CsExo70B*-OE lines than that in WT (Figure 7d). In addition, we detected significantly larger male flower and higher plant height in *CsExo70B*-OE lines (Figure S10b,c). These results suggest that *CsExo70B*-overexpressing increases fruit yield in cucumber.

On the other side, we found chitin- and flg22-induced ROS production was greatly increased in *CsExo70B* transgenic plants, especially in *CsEXO70B*-OE-4[#] and *CsEXO70B*-OE-6[#] lines (Figure 7e,f). When *CsExo70B*-OE lines and WT were simultaneously infected by a higher concentration of *Foc* spore suspension, WT plants displayed obvious stem disease symptoms, and a few of them gradually showed cotyledon wilting at 14 dpi, while *CsExo70B*-OE lines exhibited mild disease symptoms with no wilted cotyledons until 14 dpi (Figure 7g). Consistently, the DI of all the *CsExo70B*-OE lines was lower that of WT at 10 dpi and 14 dpi (Figure 7h). Similarly, *CsExo70B*-OE plants supported reduced *Psl* bacterial growth and disease spot area compared to WT (Figure 7i,j), indicating that *CsExo70B* overexpression improves pathogen resistance in cucumber.

Immunoblot analyses were further performed to detect the PM levels of RKs in *CsExo70B*-OE-4[#] and *CsExo70B*-OE-6[#] lines. Consistently, increased CsERECTA and CsLYK5 accumulation were observed at the PM in *CsExo70B*-OE lines (Figure 7k–n), and the expression of *CsERECTA*, *CsLYK5*, and *CsFLS2* was unchanged in *CsExo70B*-OE lines (Figure 7o,p, Figure S9b).
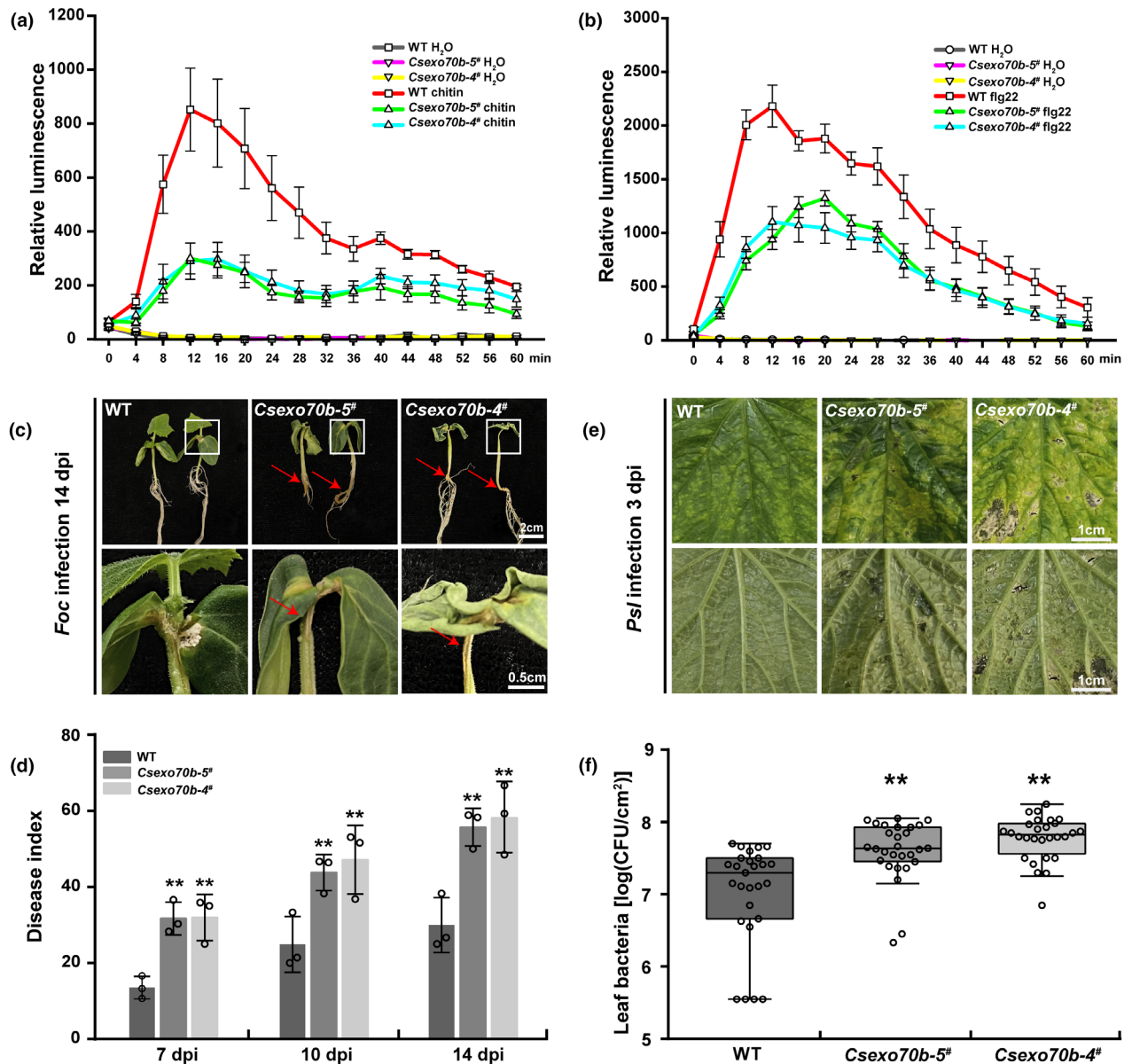
Figure 5 Knockout of *CsExo70B* compromises pathogen resistance in cucumber. (a, b) *CsExo70B* knockout lines exhibited reduced reactive oxygen species (ROS) production triggered by flg22 (a) or chitin (b). Data represent the means ± SD (*n* = 6). (c) *CsExo70B* knockout lines are more susceptible to *Fusarium oxysporum* f. sp. *Cucumerinum Owen* (*Foc*). Images were taken at 14 days post-inoculation (dpi), and the red arrows indicated wilted hypocotyls and stems. (d) Disease index (DI) in WT and *CsExo70B* knockout lines shown in (c). Data are means ± SD (*n* = 3). (e) The disease resistance phenotypes of *CsExo70B* knockout lines after inoculation with *Pseudomonas syringae* pv. *lachrymans* (*Psl*). The cucumber plants with two true leaves were spray-inoculated with *Psl*, and images were taken at 3 dpi. Scale bar = 1 cm. (f) *CsExo70B* knockout lines displayed increased susceptibility to *Psl*. Bacterial population in the leaf was measured 3 days after spray inoculation. Values are means of log (colony-forming units [CFU] cm^{-2} leaf tissue) ± SD (*n* ≥ 28). Statistical significances relative to WT are indicated by asterisks (**P < 0.01, one-way ANOVA).

Overall, these findings further support that *CsExo70B* promotes cucumber fruit elongation and disease resistances by RK levels at PM, providing a possible strategy for breeding cucumber with high yield and enhanced defence.

Discussion

When infected by pathogens, plants activate defence responses quickly and properly, but frequently penalize growth and development. Recent studies showed that the growth and

defence 'trade-off' can be uncoupled via genetic manipulations (Campos *et al*., 2016; Lu *et al*., 2022; Wang *et al*., 2014, 2018). In this study, we found that CsExo70B promotes both yield and disease resistance by regulating RKs homeostasis at PM.

Firstly, we revealed a novel function of CsExo70B in cucumber development. Previous evidence showed that the *exo70B1* mutant is smaller compared to WT in *Arabidopsis* when grown under short days for 5 weeks and exhibited hypersensitive response-like cell death and enhanced disease resistance to various pathogens (Zhao *et al*., 2015), subsequent study found
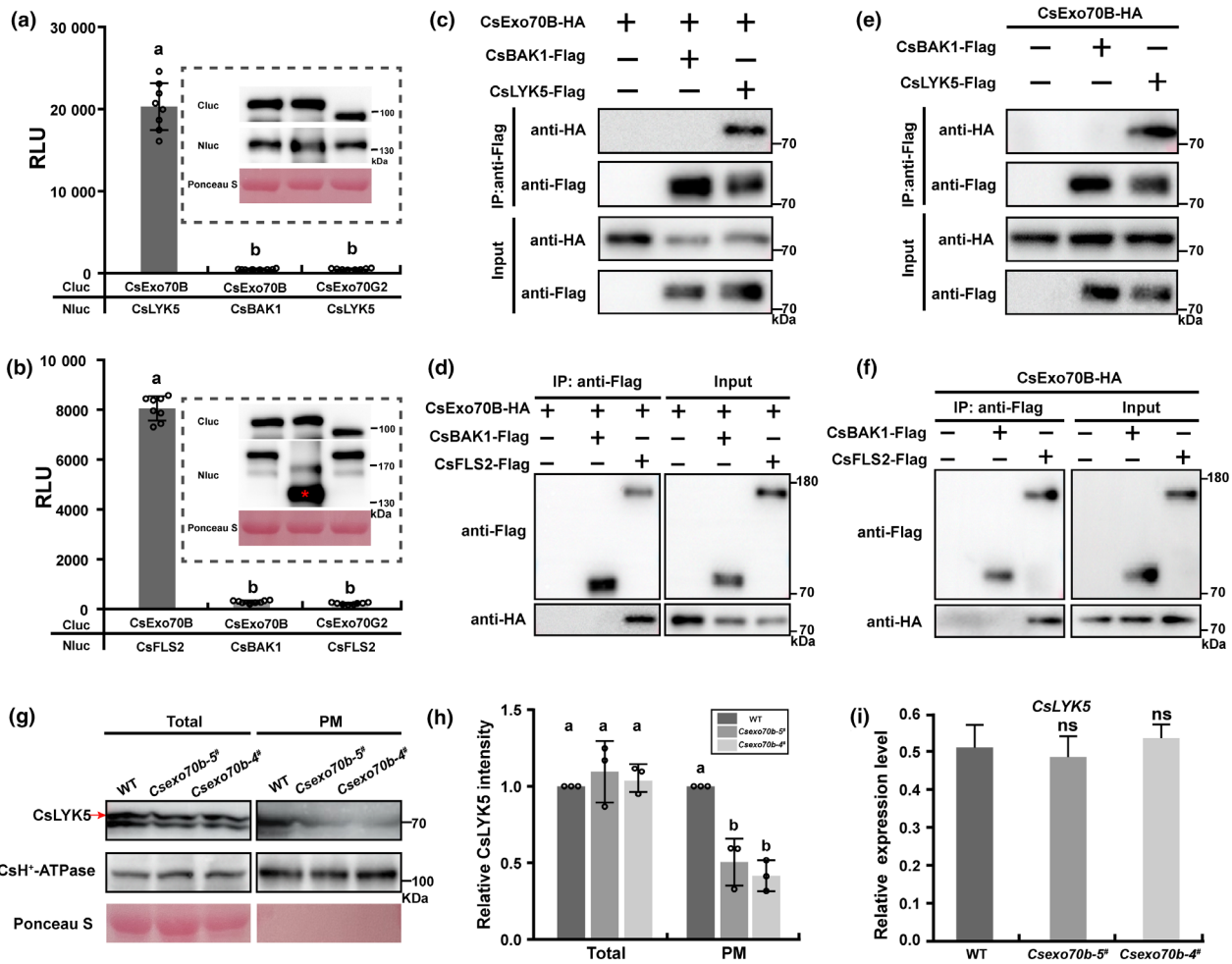
Figure 6 CsExo70B physically interacts with immune RKs and contributes to their accumulation at PM. (a, b) LUC assays indicated CsExo70B interacts with CsLYK5 (a) and CsFLS2 (b). The LUC assays were performed in *N. benthamiana* leaves by *Agrobacterium*-mediated transient expression of the indicated constructs. The relative luciferase activities were measured using a luminometer. Data are shown as means ± SD; $n = 8$. Different lower-case letters indicate statistically significant differences ($P < 0.001$, one-way ANOVA analysis with Tukey's test). (c, d) CsExo70B associates with CsLYK5 (c) and CsFLS2 (d) in *N. benthamiana*. These indicated constructs were transiently expressed in *N. benthamiana* leaves, and co-IP was performed by anti-FLAG antibody. CsBAK1-FALG was used as a negative control. (e, f) CsExo70B interacts with CsLYK5 (e) and CsFLS2 (f) in cucumber roots. The indicated constructs were expressed in hairy roots of stable *CsExo70B-HA* overexpression lines, and co-IP assays were performed with anti-FLAG antibody. (g) Immunoblotting analysis of CsLYK5 in WT and *CsExo70B* knockout lines. Total proteins were extracted from true leaves and subjected to protein fractionation. CsH+-ATPase was used as PM protein control. (h) Quantified analysis of the relative CsLYK5 levels shown in (g). The CsH+-ATPase protein was used as control. Data represent means ± SD of three independent experiments. Different lowercase letters indicate statistically significant differences ($P < 0.05$, one-way ANOVA analysis with Tukey's test). (i) The levels of *CsLYK5* transcript were normal in WT and *Csexo70b* mutants. Data are means ± SD, $n = 3$ (ns, no significant difference, one-way ANOVA).

that these phenotypes of *exo70B1* was caused by constitutive activation of an atypical intracellular immune receptor TIR-NBS2 (TN2) (Zhao *et al.*, 2015). Thus, the development defect of *exo70B1* mutant in *Arabidopsis* is due to constitutive immune activation, and Exo70B was not considered as a real developmental regulator. Interestingly, the cucumber *exo70b* mutants displayed shorter fruits and slightly reduced plant height (Figure 1, Figure S1). However, it seems that the developmental defects were not caused by constitutive immune activation, because no cell death was observed in *Csexo70b* mutants (Figure S11a), and the expression of pathogenesis-related genes *CsPR1* and *CsPR2* also exhibited normal in *Csexo70b* mutants (Figure S11b,c). Besides, *Csexo70b* mutants showed more susceptible rather than resistance to pathogens (Figure 5). In addition, previous study

reported that there are only two genes encoding TIR-NBSs in cucumber, and both of them have low similarity to TN2 in sequences (Wan *et al.*, 2013). Therefore, our evidences demonstrated that CsExo70B directly regulates cucumber development.

Due to Exo70B has been linked to the trafficking of immune RKs to the PM in previous studies (Hou *et al.*, 2020; Wang *et al.*, 2020a). The short fruit phenotype of *Csexo70b* mutants reminds us of ERECTA, which mutation led to short siliques in *Arabidopsis* (Pillitteri *et al.*, 2007; Shpak *et al.*, 2003). As expected, the fruit length and plant height were greatly reduced in *Cserecta* mutants generated by CRISPR/Cas9 system (Figure 2, Figure S3). Our extensive analyses found that CsExo70B interacts with CsERECTA and regulates its accumulation at the PM in fruit tissue (Figure 3). Consistently, the fruit length of the *Csexo70b*

Cserecta double mutant is similar to that of *Cserecta* mutant rather than *Csexo70b* mutant (Figure 4a–d), indicating that *CsERECTA* acted genetically downstream of *CsExo70B*. Notably, the short-fruit phenotype of *Cserecta* was more severe than that of *Csexo70b* (Figures 1, 2 and 4), which is plausible considering that CsExo70B regulating CsERECTA's accumulation at the PM, thus knockout of *CsExo70B* exhibited only partial phenotype of *Cserecta*. Moreover, the RNA-seq analysis demonstrated that 76.5% transcripts were co-regulated by *CsExo70B* and *CsERECTA*

(Figure 4e–i), indicating that CsExo70B and CsERECTA regulate fruit elongation in the same pathway in cucumber. Among the down-regulated DEGs, YUCC4 and other auxin- and cell division-responsive factors were significantly decreased (Figure S12), implying that the shorter fruits in *Csexo70b* and *Cserecta* mutants may be mediated by plant hormone pathways. Furthermore, CsExo70B interacts with CsCLV1 (Figure S2), which mutation leads to an increased carpel number in cucumber (Cheng *et al.*, 2022). The increased carpel number was also observed in
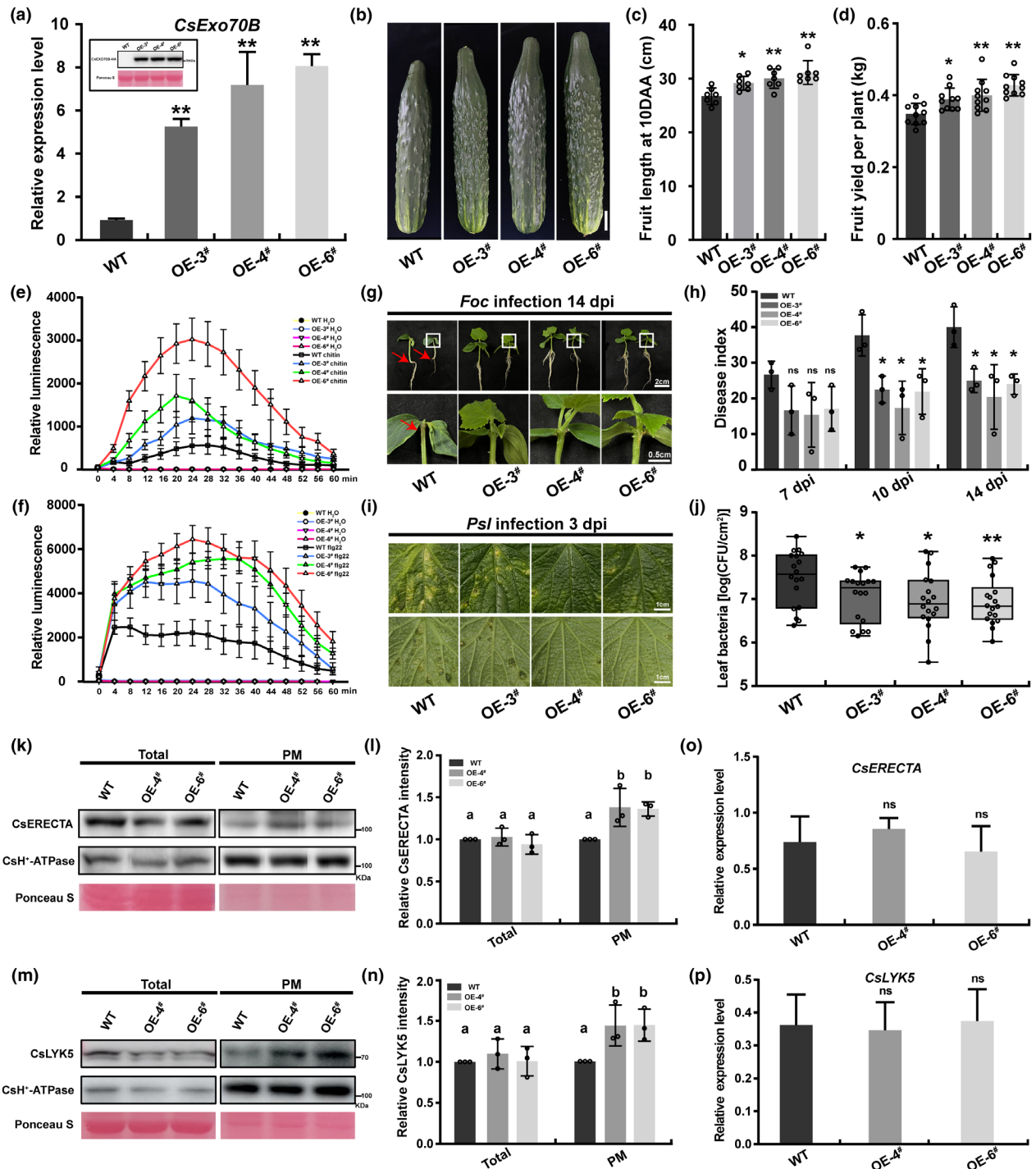
Figure 7 Overexpression of *CsExo70B* enhances fruit yield and resistance to pathogens in cucumber. (a) The identification of *CsExo70B*-OE lines. Transcripts of *CsExo70B* were detected by qRT-PCR. Data are shown as means ± SD (n = 3). Statistical significances were determined by one-way ANOVA (**P < 0.01). The gels shown the protein levels of CsExo70B detected by anti-HA immunoblot. Equal loading was demonstrated by Ponceau S of Rubisco. (b) Morphology of cucumber fruit at 10 DAA of WT and *CsExo70B*-OE lines. Scale bar = 3 cm. (c) The length of fruits at 10 DAA shown in (b) was quantified. Data are shown as means ± SD, n = 11 (*P < 0.05; **P < 0.01, one-way ANOVA). (d) Fruit yield per plant in WT and *CsExo70B*-OE lines. Data represent as mean ± SD, n = 10 individual plants (*P < 0.05, **P < 0.01, one-way ANOVA). (e, f) chitin (e) and flg22 (f) triggered ROS production in *CsExo70B*-OE lines. Data represent the means ± SD (n = 8). (g) The seedling morphology of WT and *CsExo70B*-OE lines at 14 dpi with *Foc*. White boxes indicate 'zoomed-in' regions. (h) The DI of WT and *CsExo70B*-OE lines shown in (g). Data represent the means ± SD, n = 3. (*P < 0.05, one-way ANOVA). (i, j) *CsExo70B*-OE lines confer resistance to *Psl*. The cucumber plants with two true leaves were spray-inoculated with *Psl*, and the disease resistance phenotypes were collected at 3 dpi. Values are means of log ([CFU] cm^{-2} leaf tissue) ± SD; n = 18. Significant differences relative to WT are indicated by asterisks (*P < 0.05; **P < 0.01 one-way ANOVA). (k) Immunoblotting analysis of CsERECTA levels in WT and *CsExo70B*-OE lines. Ponceau S was used as protein loading control. (l) Quantified analysis of relative CsERECTA levels in WT and *CsExo70B*-OE lines. The relative protein band density of CsERECTA was normalized to that of CsH$^+$-ATPase. Data represent means ± SD of three independent experiments. Different lower-case letters indicate statistically significant differences (P < 0.05, one-way ANOVA analysis with Tukey's test). (m) Immunoblotting analysis of CsLYK5 levels in *CsExo70B*-OE lines. Total proteins and PM proteins were extracted from leaves and detected by anti-CsLYK5 antibody. (n) Quantified analysis of the relative CsLYK5 levels shown in (m). The CsH$^+$-ATPase levels were used as normalization standard. Data are presented as mean ± SD of three independent experiments. Different lowercase letters indicate statistically significant differences (P < 0.05, one-way ANOVA analysis with Tukey's test). (o, p) Transcript analyses of *CsERECTA* (o) and *CsLYK5* (p) in *CsExo70B*-OE lines. Data are means ± SD, n = 3 (ns, no significant difference, one-way ANOVA).

Csexo70b mutants (Figure 1d,g). It is speculated that CsExo70B may regulate carpel number via modulating CLV1 accumulation at the PM in cucumber.

Secondly, previous studies have shown that Exo70B1 and Exo70B2 are involved in resistances to fungal and bacterial pathogens, which cause leaf disease in rice and *Arabidopsis* (Hou *et al.*, 2020; Pecenková *et al.*, 2011). Our analyses found that cucumber *Csexo70b* mutant exhibited more susceptible to *Psl* infection in leaves (Figure 5e,f). Not only that, *Csexo70b* mutant also displayed reduced resistance to vascular pathogen *Foc* (Figure 5c,d), which causes wilt in cucumber, indicating cucumber resistance to leaf and vascular pathogens both depends on CsExo70B. Similarly, CsExo70B also interacts with immune RKs CsFLS2 and CsLYK5 and promotes their accumulation at the PM in cucumber (Figure 6). Consistent with the reduced immune RK levels at the PM, the RK-mediated ROS production was compromised in *Csexo70b* mutants (Figure 5a,b). Together, these results suggest CsExo70B provides a broad-spectrum resistance to different pathogens through regulating the accumulation of immune RKs at the PM.

Moreover, we found that the cucumber plants with higher yield and stronger defence can be achieved simultaneously by overexpression of *CsExo70B* (Figure 7), indicating that CsExo70B acts as an integral component to promote both fruit elongation and defence response in cucumber. However, the molecular mechanism underlying CsExo70B regulates growth-defence tradeoffs is unknown. Several plausible mechanisms may explain the switch of growth to defence. One possibility is that CsExo70B may function in an organ- or tissue-specific manner. Our results showed that *CsERECTA* was specifically highly expressed in fruit, while both *CsFLS2* and *CsLYK5* were significantly lower expressed in fruit than other tissues (Figure S13). When infected by pathogens, the expression levels of *CsExo70B* (Liu *et al.*, 2023) and immune *RKs* (*CsFLS2* and *CsLYK5*) were significantly up-regulated, but the expression of *CsERECTA* was markedly down-regulated in roots and leaves rather than fruits (Figures S14 and S15). So, one possibility is that CsExo70B may preferentially promote CsERECTA accumulation in fruit to regulate fruit elongation; while CsExo70B may have a prior choice to traffic more immune RKs to PM to activate stronger defence in roots and leaves upon pathogen attack. In addition, previous study

showed IPA1 promotes disease resistance and yield by activating different genes through reversible phosphorylation (Wang *et al.*, 2018). So, another possibility that cannot be ruled out is CsExo70B may also have different post-translational modification states before and after pathogen infection, and select to traffic different RKs to enhance fruit length and disease resistance.

Collectively, the data presented here reveal a regulatory mechanism that CsExo70B positively regulates fruit elongation and disease resistances via fine-tuning the PM accumulation of CsERECTA and CsLYK5 in cucumber (Figure 8). In field, cucumber is often challenged by various pathogens, resulting in reduced production. In the future, fine tuning the expression level of *Exo70B* will provide a promising breeding strategy with high yield and robust defence in cucumber and other species.

Experimental procedures

Plant materials and growth conditions

Cucumber (*Cucumis sativus* L.) inbred line XTMC was used in this study for genetic transformation, pathogen infection assays, and expression analysis. The cucumber seedlings at three true-leaf stage were transplanted to the greenhouse with standard water and fertilizer management and pest control in China Agricultural University, Beijing. The *N. bethamiana* was grown in a growth chamber set at 24 °C with 16-h-light/8-h-dark, and the 5-week-old plants were used for protein–protein interaction analysis.

Cucumber transformation

To generate *Csexo70b* and *Cserecta* mutants using the CRISPR/Cas9 system, the single-guide RNA (sgRNA) target sites of *CsExo70B* and *CsERECTA* were selected by the sgRNA design web (http://crispr.hzau.edu.cn/CRISPR2/). The corresponding guide RNAs were cloned into pKSE402G, which contained a green fluorescent protein (GFP) reporter (Hu *et al.*, 2017; Xing *et al.*, 2014). To generate *CsExo70B* overexpression transgenic plants, the full-length coding sequence of *CsExo70B* without termination codon was first cloned into PUC19-35S-HA vector, and then, the full length of *CsExo70B-HA* was cloned into pCAMBIA1305.4 vector, which contained a 35S-GFP expression cassette and a 35S-GUS expression cassette, SmaI and BstEII sites were selected for replacing GUS to *CsExo70B-HA*. All the
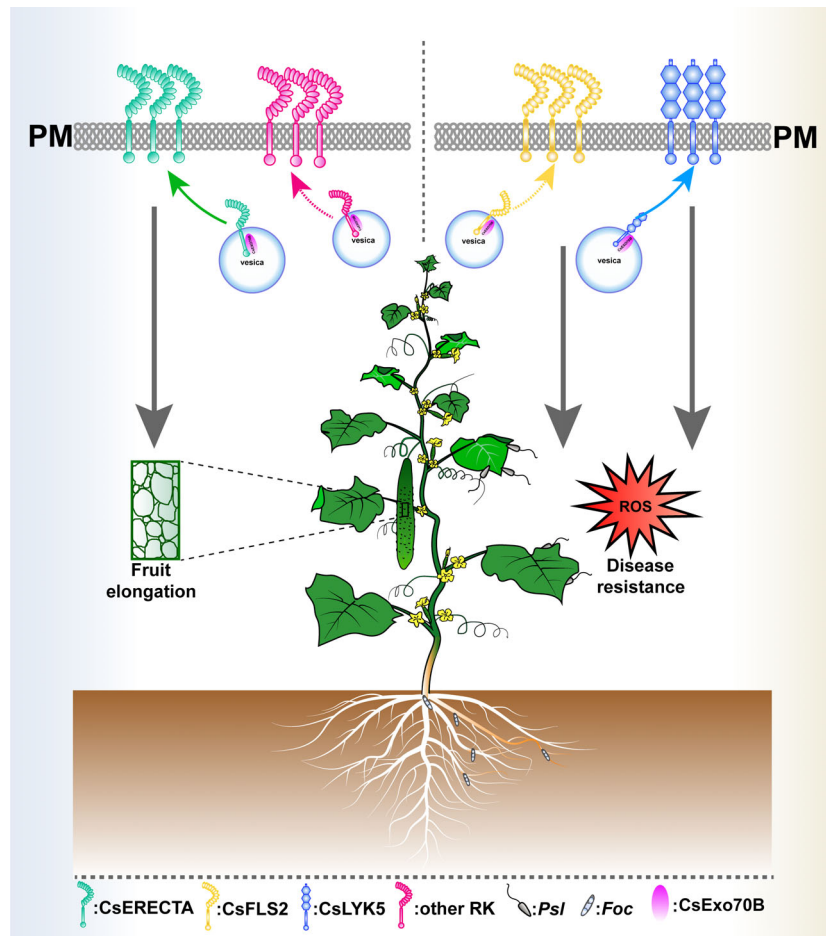
Figure 8 The working model for CsExo70B promotes fruit elongation and pathogen resistance in cucumber. In cucumber, the exocyst subunit CsExo70B interacts with the developmental RK CsERECTA and maintains the level of CsERECTA at PM, promoting fruit elongation. On the other hand, CsExo70B also associates with immune RKs CsFLS2 and CsLYK5 and contributes their accumulation at the PM for resistance to pathogens.

resulting constructs were transferred into the *Agrobacterium tumefaciens* strain EHA105, and the cucumber transformation was performed as described previously (Hu *et al.*, 2017).

All positive T_0 transgenic plants were selected by GFP reporter. The *CsExo70B* and *CsERECTA* mutated lines were genotyped by PCR using gene-specific primers, and the *CsExo70B* overexpression transgenic lines were detected by immunoblot using anti-HA antibodies. All primers used in cucumber transformation are shown in Table S4.

Measurements of the cell length and cell number

The cucumber fruits at 10 DAA were fixed in 3.7% FAA (50 mL Ethanol, 5 mL Acetic acid, 10 mL 37% Formaldehyde, 35 mL Ultrapure H_2O) solution. 1-cm-thick slices from cucumber fruit pericarp were embedded, sectioned, dewaxed, and stained with toluidine blue. Finally, the sections were observed under a microscope (Olympus DP72, Japan), and the cell length and cell number along a longitudinal axis were quantified using the ImageJ software.

ROS production assays

ROS assays were performed in cucumber plants as described previously in *Arabidopsis* (Zhang *et al.*, 2007) with some modification. Leaf discs were collected from the second true

leaves of cucumber seedlings (two discs per leaf), placed into the white 96-well plate with 200 μL sterile water overnight and then removed the water and treated with 100 nM flg22 or 0.2 mg mL^{-1} chitin in 200 μL of buffer containing 100 μM luminol and 10 μg mL^{-1} horseradish peroxidase. Luminescence was immediately detected with a luminometer (Tecan Infinite F200).

Pathogen infection assays

Pseudomonas syringae pv. *lachrymans* (*Psl*) were cultured in King's medium B (King *et al.*, 1954) at 28 °C. Leaves of the cucumber seedlings at two-three true leaf stage were sprayed with *Psl* at 1×10^8 CFU mL^{-1}, containing 0.017% Silwet L-77, and bacterial number in leaves was determined 3 days post-inoculation (dpi). One leaf discs served as one replicate, and each data point represented at least 18 replicates from at least 6 plants for each genotype (Zhang *et al.*, 2010).

Fusarium oxysporum f. sp. *Cucumerinum Owen* (*Foc*) stain was grown on potato dextrose agar (PDA) (Difco™) for 7–10 days at 27 °C, then the hyphae were transferred into Armstrong Fusarium liquid Medium on a shaker (25 °C; 150 rpm; 5 days) for sporulation. The spores were harvested and then adjusted to an inoculated concentration of 1×10^6 spores/mL for *Csexo70b* mutants and 5×10^6 spores/mL for *CsExo70B*-OE lines. The

cucumber seedlings with 1 cm radicles were inoculated with the spore suspension for 1 h. Finally, the infected seedlings were planted in sterilized soil at 25 °C and 80% relative humidity with a 16-h-light/8-h-dark photoperiod. The severity of disease symptoms of each cucumber seedling was graded from 0 to 4, where 0 = no symptoms, 1 = cotyledons or stems lose lustre with mild symptoms, 2 = one cotyledon wilted, 3 = two cotyledons and stem severely wilted, 4 = the whole plant wilted and died. The disease index (DI) was recorded and calculated using a previously described method with minor modifications (Wang *et al.*, 2020b), and all infection experiments were repeated three to four times.

RNA extraction and qRT-PCR

Total RNA was isolated using the Eastep® Super Total RNA Extraction Kit (Promega) according to the manufacturer's instructions, and 1.2 μg total RNA was reverse-transcribed using a FastKing gDNA Dispelling RT SuperMix Kit (Tiangen). All qRT-PCR assays were performed using TB Green® Premix Ex Taq™ II (Takara) in a CFX384 Real-Time PCR System (BIO-RAD). The cucumber *Ubiquitin* gene (*CsaV3_5G031430*) was used as a reference, and the relative expression levels were calculated using the $2^{-\Delta\Delta Ct}$ method (Livak and Schmittgen, 2001). Three biological replicates and three technical replicates were performed (Wan *et al.*, 2010).

For determination of the expression levels of *CsERECTA*, *CsFLS2* and *CsLYK5* in indicated genotypes, RNA was extracted from 15-day-old cucumber seedlings. For analyses of *PsI*-inducible gene expression, cucumber seedlings at two-three true leaf stage were spray-inoculated with *PsI*, and leaves were collected at 0, 1, 2, 3 dpi for RNA extraction. For analyses of *Foc*-inducible gene expression, roots were collected at 0, 2, 4, and 6 dpi by *Foc* for RNA extraction. All primer sequences for qRT-PCR are listed in Table S4.

Split-luciferase complementation assays

The CDSs of *CsExo70B* and *CsExo70G2* were cloned into pCAMBIA1300-CLuc vector, and the CDSs of *CsERECTA*, *CsFLS2*, *CsLYK5*, *CsBAK1*, *CsFERONIA* and *CsCLV1* without stop codons were amplified and inserted into pCAMBIA1300-HA-NLuc vector, respectively. These above constructs were then transferred into the *A. tumefaciens* strain GV3101 and co-infiltrated into *N. benthamiana* leaves as described previously (Zhou *et al.*, 2018). After 40–48 h infiltration, the relative luciferase activity was recorded in a 96-well plate using a luminometer (Tecan Infinite F200) as described previously (Zhou *et al.*, 2018). These Cluc- and Nluc-fusion proteins were detected by anti-Cluc (Sigma-Aldrich) anti-HA (CWBIO) antibodies, respectively.

Co-immunoprecipitation (IP) assays

Full-length coding sequence without stop codon of *CsExo70B* was cloned into pCAMBIA1300-35S-HA, and *CsERECTA*, *CsFLS2*, *CsLYK5* and *CsBAK1* were cloned into pCAMBIA1300-35S-FLAG vector. For Co-IP assays in *N. benthamiana* leaves, these resulting plasmids were transferred into the *A. tumefaciens* strain GV3101 and transient expressed as previously described (Shi *et al.*, 2013; Zhou *et al.*, 2018). For co-IP assays in cucumber, these constructs including CsERECTA-FLAG, CsFLS2-FLAG, CsLYK5-FLAG and CsBAK1-FLAG were transferred into the *A. rhizogenes* strain K599 and infiltrated the hypocotyl of transgenic 35S:*CsExo70B*-HA plants to induce hairy roots for protein extraction as previously described (Yao *et al.*, 2023). Total protein was extracted with the

protein extraction buffer (50 mM HEPES [pH 7.5], 150 mM KCl, 1 mM EDTA [pH 8.0], 1 mM DTT, 0.05% (v/v)Triton X-100, 1× protease inhibitor cocktail [Roche]) and incubated with agarose conjugated anti-FLAG antibody (Sigma-Aldrich) for 1–2 h at 4 °C. The beads were washed 5–6 times with the protein extraction buffer. The bound protein was eluted with 0.5 mg/mL 3× FLAG (Sigma-Aldrich) for 0.5 h at 4°C and separated by SDS-PAGE and detected using anti-HA (CWBIO) and anti-FLAG (Sigma-Aldrich) antibodies.

Bimolecular fluorescence complementation (BiFC) assays

Full-length coding sequences of *CsExo70B*, *CsERECTA*, *CsFLS2* and *CsLYK5* without stop codons were cloned and inserted into *pSPYCE-35S* and *pSPYNE-35S* vectors carrying the N-terminal/C-terminal half of Yellow Fluorescent Protein (YFP) expression fragment (Walter *et al.*, 2004). These constructs were transiently expressed in *N. benthamiana* leaves and were performed as previously described (Zhou *et al.*, 2018), YFP signals were imaged by confocal imaging (Olympus BX51, Japan) under 488 nm excitation wavelength at 72 h post-infiltration. The primers used are listed in Table S4.

Antibody production

CsERECTA, CsLYK5 and CsH⁺-ATPase specific antibodies were produced against the peptides CTKRQPSDRPTMHE, TRAKGMDS-KIDKNM and IKNEAVDLEHIPIE by GenScript (www.genscript.com), respectively. Specificity of CsERECTA antibody was tested using *Cserecta* knockout mutants and *N. benthamiana* expressing CsERECTA-FLAG, and CsLYK5 antibody was detected by cucumber total protein or CsLYK5-FLAG protein expressed in *N. benthamiana*, and CsH⁺-ATPase antibody was verified by cucumber total protein and plasma membrane protein.

Plasma membrane (PM) protein fractionation and immunoblotting assays

The PM protein was extracted from cucumber fresh true leaves or ovaries using a Minute™ Plant Plasma Membrane Protein Isolation Kit (Invent Biotechnologies) according to the instruction and operation manual. Immunoblotting analysis of endogenous levels of CsERECTA, CsLYK5 and CsH⁺-ATPase was detected with synthetic endogenous antibodies.

RNA sequencing and data analysis

For RNA-seq analysis, ovaries at 3 DAA of WT, *Csexo70b-5#* and *Cserecta-2#* mutants were collected for RNA extraction and subjected to RNA-Seq analysis. Three ovaries were collected from different plants as one biological repeat, and three biological repeats were performed. RNA library construction and sequencing were performed on the Illumina HiSeq X-ten platform by Biomarker Technologies Corporation (www.biomarker.com.cn).

Clean read pairs were mapped to reference cucumber genome (Chinese long v.3.0). DEGs were identified via fragments per kilobase of transcript per million mapped fragments (FPKM) on the BMKCloud online platform (Fold change ≥ 2.0, FDR < 0.01), the heat maps were generated via TBtools Software (Chen *et al.*, 2020).

Statistical analysis

All experiments were repeated at least three times. Data were analysed on GraphPad Prism9 with two-tailed Student's *t* test for comparison between two samples, and one-way ANOVA Tukey's test for pairwise comparisons among multiple samples.

Conflict of interest

The authors declare no competing interests.

Accession numbers

Sequence data in this article can be found in Cucurbit Genomics Database (http://www.cucurbitgenomics.org/); all the accession numbers of genes are listed in Table S5.

Author contributions

X.Z., Z.Z. and L.L. designed experiments. L.L. performed the majority of the experiments and analysed the data. L.L., Z.Z. and X.Z. wrote this manuscript. J.C. C.G., S.W., Y.X., L.H., W.S. and J.Z. provided experimental assistances. Z.Z., Z.W. and X.L. provided technical guidance. M.L., C.L. and L.W. checked this manuscript. All authors discussed the results and contributed to this manuscript.

References

Amano, Y., Tsubouchi, H., Shinohara, H., Ogawa, M. and Matsubayashi, Y. (2007) Tyrosine-sulfated glycopeptide involved in cellular proliferation and expansion in *Arabidopsis*. *Proc. Natl. Acad. Sci. USA*, **104**, 18333–18338.

Campos, M.L., Yoshida, Y., Major, I.T., de Oliveira Ferreira, D., Weraduwage, S.M., Froehlich, J.E., Johnson, B.F. *et al.* (2016) Rewiring of jasmonate and phytochrome B signalling uncouples plant growth–defense tradeoffs. *Nat. Commun.* **7**, 12570.

Cao, Y., Liang, Y., Tanaka, K., Nguyen, C.T., Jedrzejczak, R.P., Joachimiak, A. and Stacey, G. (2014) The kinase LYK5 is a major chitin receptor in *Arabidopsis* and forms a chitin-induced complex with related kinase CERK1. *Elife*, **3**, e03766.

Chand, J.N. and Walker, J.C. (1964) Inheritance of resistance to angular leaf spot of cucumber. *Phytopathology*, **54**, 51–53.

Che, G., Song, W.Y. and Zhang, X.L. (2023) Gene network associates with CsCRC regulating fruit elongation in cucumber. *Vegetable Research*, **3**, 7.

Chen, C., Chen, H., Zhang, Y., Thomas, H.R., Frank, M.H., He, Y. and Xia, R. (2020) TBtools: an integrative toolkit developed for interactive analyses of big biological data. *Mol. Plant*, **13**, 1194–1202.

Cheng, F., Song, M., Zhang, M., Cheng, C., Chen, J. and Lou, Q. (2022) A SNP mutation in the *CsCLAVATA1* leads to pleiotropic variation in plant architecture and fruit morphogenesis in cucumber (*Cucumis sativus* L.). *Plant Sci.* **323**, 111397.

Choi, S.W., Tamaki, T., Ebine, K., Uemura, T., Ueda, T. and Nakano, A. (2013) RABA members act in distinct steps of subcellular trafficking of the FLAGELLIN SENSING2 receptor. *Plant Cell*, **25**, 1174–1187.

Chong, Y.T., Gidda, S.K., Sanford, C., Parkinson, J., Mullen, R.T. and Goring, D.R. (2010) Characterization of the *Arabidopsis thaliana* exocyst complex gene families by phylogenetic, expression profiling, and subcellular localization studies. *New Phytol.* **185**, 401–419.

Clark, S.E., Williams, R.W. and Meyerowitz, E.M. (1997) The *CLAVATA1* gene encodes a putative receptor kinase that controls shoot and floral meristem size in *Arabidopsis*. *Cell*, **89**, 575–585.

Coley, P.D., Bryant, J.P. and Chapin, F.S. (1985) Resource availability and plant antiherbivore defense. *Science*, **230**, 895–899.

Couto, D. and Zipfel, C. (2016) Regulation of pattern recognition receptor signalling in plants. *Nat. Rev. Immunol.* **16**, 537–552.

Dong, J., Xu, J., Xu, X., Xu, Q. and Chen, X. (2019) Inheritance and quantitative trait locus mapping of *Fusarium* wilt resistance in cucumber. *Front. Plant Sci.* **10**, 1425.

Drdová, E.J., Synek, L., Pečenková, T., Hála, M., Kulich, I., Fowler, J.E., Murphy, A.S. *et al.* (2013) The exocyst complex contributes to PIN auxin efflux carrier recycling and polar auxin transport in *Arabidopsis*. *Plant J.* **73**, 709–719.

Gust, A.A., Pruitt, R. and Nurnberger, T. (2017) Sensing danger: key to activating plant immunity. *Trends Plant Sci.* **22**, 779–791.

Gómez, G.L. and Boller, T. (2000) FLS2: an LRR receptor-like kinase involved in the perception of the bacterial elicitor flagellin in *Arabidopsis*. *Mol. Cell*, **5**, 1003–1011.

He, Z., Webster, S. and He, S.Y. (2022) Growth-defense trade-offs in plants. *Curr. Biol.* **32**, R634–R639.

Herms, D.A. and Mattson, W.J. (1992) The dilemma of plants: to grow or defend. *Q. Rev. Biol.* **67**, 283–335.

Hou, H., Fang, J., Liang, J., Diao, Z., Wang, W., Yang, D., Li, S. *et al.* (2020) *OsExo70B1* positively regulates disease resistance to *Magnaporthe oryzae* in rice. *Int. J. Mol. Sci.* **21**, 7049.

Hu, B., Li, D., Liu, X., Qi, J., Gao, D., Zhao, S., Huang, S. *et al.* (2017) Engineering non-transgenic gynoecious cucumber using an improved transformation protocol and optimized CRISPR/Cas9 system. *Mol. Plant*, **10**, 1575–1578.

Huot, B., Yao, J., Montgomerya, B.L. and He, S.Y. (2014) Growth–defense tradeoffs in plants: a balancing act to optimize fitness. *Mol. Plant*, **7**, 1267–1287.

King, E.O., Ward, M.K. and Raney, D.E. (1954) Two simple media for the demonstration of pyocyanin and fluorescin. *J. Lab. Clin. Med.* **44**, 301–307.

Kinoshita, A., Betsuyaku, S., Osakabe, Y., Mizuno, S., Nagawa, S., Stahl, Y., Simon, R. *et al.* (2010) RPK2 is an essential receptor-like kinase that transmits the CLV3 signal in *Arabidopsis*. *Development*, **137**, 3911–3920.

Kulich, I., Vojtíková, Z., Glanc, M., Ortmannová, J., Rasmann, S. and Žárský, V. (2015) Cell wall maturation of *Arabidopsis* trichomes is dependent on exocyst subunit EXO70H4 and involves callose deposition. *Plant Physiol.* **168**, 120–131.

Kulich, I., Vojtíková, Z., Sabol, P., Ortmannová, J., Neděla, V., Tihlaříková, E. and Žárský, V. (2018) Exocyst subunit EXO70H4 has a specific role in callose synthase secretion and silica accumulation. *Plant Physiol.* **176**, 2040–2051.

Lee, H.Y., Bowen, C.H., Popescu, G.V., Kang, H.G., Kato, N., Ma, S., Dinesh-Kumar, S. *et al.* (2011) *Arabidopsis* RTNLB1 and RTNLB2 reticulon-like proteins regulate intracellular trafficking and activity of the FLS2 immune receptor. *Plant Cell*, **23**, 3374–3391.

Liang, X. and Zhou, J.M. (2018) Receptor-like cytoplasmic kinases: central players in plant receptor kinase–mediated signaling. *Annu. Rev. Plant Biol.* **69**, 267–299.

Liu, L., Gu, C.H., Zhang, J.H., Guo, J.Y., Zhang, X.L. and Zhou, Z.Y. (2023) Genome-wide analysis of exocyst complex subunit *Exo70* gene family in cucumber. *Int. J. Mol. Sci.* **24**, 10929.

Livak, K.J. and Schmittgen, T.D. (2001) Analysis of relative gene expression data using real-time quantitative PCR and the $2^{-\Delta\Delta C_T}$ method. *Methods*, **25**, 402–408.

Lu, K., Chen, X., Yao, X., An, Y., Wang, X., Qin, L., Li, X. *et al.* (2022) Phosphorylation of a wheat aquaporin at two sites enhances both plant growth and defense. *Mol.Plant.* **15**, 1772–1789.

Matsubayashi, Y. (2014) Posttranslationally modified small-peptide signals in plants. *Annu. Rev. Plant Biol.* **65**, 385–413.

Matsubayashi, Y., Ogawa, M., Morita, A. and Sakagami, Y. (2002) An LRR receptor kinase involved in perception of a peptide plant hormone, phytosulfokine. *Science*, **296**, 1470–1472.

Morris, E.R. and Walker, J.C. (2003) Receptor-like protein kinases: the keys to response. *Curr. Opin. Plant Biol.* **6**, 339–342.

Pan, Y., Liang, X., Gao, M., Liu, H., Meng, H., Weng, Y. and Cheng, Z. (2017) Round fruit shape in WI7239 cucumber is controlled by two interacting quantitative trait loci with one putatively encoding a tomato *SUN* homolog. *Theor. Appl. Genet.* **130**, 573–586.

Pecenková, T., Hála, M., Kulich, I., Kocourková, D., Drdová, E., Fendrych, M., Toupalová, H. *et al.* (2011) The role for the exocyst complex subunits Exo70B2 and Exo70H1 in the plant-pathogen interaction. *J. Exp. Bot.* **62**, 2107–2116.

Pillitteri, L., Bemis, S., Shpak, E. and Torii, K. (2007) Haploinsufficiency after successive loss of signaling reveals a role for *ERECTA*-family genes in *Arabidopsis* ovule development. *Development*, **134**, 3099–3109.

Saeed, B., Brillada, C. and Trujillo, M. (2019) Dissecting the plant exocyst. *Curr. Opin. Plant Biol.* **52**, 69–76.

Shi, H., Shen, Q., Qi, Y., Yan, H., Nie, H., Chen, Y., Zhao, T. *et al.* (2013) BR-SIGNALING KINASE1 physically associates with FLAGELLIN SENSING2 and regulates plant innate immunity in *Arabidopsis*. *Plant Cell*, **25**, 1143–1157.

Shiu, S.H. and Bleecker, A.B. (2001a) Plant receptor-like kinase gene family: diversity, function, and signaling. *Sci. STKE*, **2001**, re22.

Shiu, S.H. and Bleecker, A.B. (2001b) Receptor-like kinases from *Arabidopsis* form a monophyletic gene family related to animal receptor kinases. *Proc. Natl. Acad. Sci. USA*, **98**, 10763–10768.

Shpak, E.D. (2013) Diverse roles of *ERECTA* family genes in plant development. *J. Integr. Plant Biol.* **55**, 1238–1250.

Shpak, E.D., Lakeman, M.B. and Torii, K.U. (2003) Dominant-negative receptor uncovers redundancy in the *Arabidopsis* ERECTA leucine-rich repeat receptor–like kinase signaling pathway that regulates organ shape. *Plant Cell*, **15**, 1095–1110.

Stegmann, M., Anderson, R.G., Ichimura, K., Pecenkova, T., Reuter, P., Žárský, V., McDowell, J.M. *et al.* (2012) The ubiquitin ligase PUB22 targets a subunit of the exocyst complex required for PAMP-triggered responses in *Arabidopsis*. *Plant Cell*, **24**, 4703–4716.

Stegmann, M., Anderson, R.G., Westphal, L., Rosahl, S., McDowell, J.M. and Trujillo, M. (2013) The exocyst subunit *Exo70B1* is involved in the immune response of *Arabidopsis thaliana* to different pathogens and cell death. *Plant Signal. Behav.* **8**, e27421.

Synek, L., Schlager, N., Eliás, M., Quentin, M., Hauser, M.T. and Zárský, V. (2006) AtEXO70A1, a member of a family of putative exocyst subunits specifically expanded in land plants, is important for polar growth and plant development. *Plant J.* **48**, 54–72.

TerBush, D.R., Maurice, T., Roth, D. and Novick, P. (1996) The exocyst is a multiprotein complex required for exocytosis in *Saccharomyces cerevisiae*. *EMBO J.* **15**, 6483–6494.

Walter, M., Walter, M., Chaban, C., Schütze, K., Batistic, O., Weckermann, K., Näke, C. *et al.* (2004) Visualization of protein interactions in living plant cells using bimolecular fluorescence complementation. *Plant J.* **40**, 428–438.

Wan, H., Yuan, W., Bo, K., Shen, J., Pang, X. and Chen, J. (2013) Genome-wide analysis of NBS-encoding disease resistance genes in *Cucumis sativus* and phylogenetic study of NBS-encoding genes in Cucurbitaceae crops. *BMC Genomics*, **14**, 109.

Wan, H., Zhao, Z., Qian, C., Sui, Y., Malik, A.A. and Chen, J. (2010) Selection of appropriate reference genes for gene expression studies by quantitative real-time polymerase chain reaction in cucumber. *Anal. Biochem.* **399**, 257–261.

Wang, J., Wang, J., Zhou, L., Shi, H., Chern, M., Yu, H., Yi, H. *et al.* (2018) A single transcription factor promotes both yield and immunity in rice. *Science*, **361**, 1026–1028.

Wang, W., Liu, N., Gao, C., Cai, H., Romeis, T. and Tang, D. (2020a) The *Arabidopsis* exocyst subunits EXO70B1 and EXO70B2 regulate FLS2 homeostasis at the plasma membrane. *New Phytol.* **227**, 529–544.

Wang, P., Zhou, L., Jamieson, P., Zhang, L., Zhao, Z., Babilonia, K., Shao, W. *et al.* (2020b) The cotton wall-associated kinase GhWAK7A mediates responses to fungal wilt pathogens by complexing with the chitin sensory receptors. *Plant Cell*, **32**, 3978–4001.

Wang, Y., Cheng, X., Shan, Q., Zhang, Y., Liu, J., Gao, C. and Qiu, J.L. (2014) Simultaneous editing of three homoeoalleles in hexaploid bread wheat confers heritable resistance to powdery mildew. *Nat. Biotechnol.* **32**, 947–951.

Weng, Y. and Wehner, T.C. (2017) Cucumber gene catalogue 2017. In: *Cucurbit Genetic Cooperative* (Grumet, R., Crosby, K., Wehner, T., Myers, J., Behera, T., eds), pp 17–29. Charleston: Vegetable Laboratory.

Xing, H.L., Dong, L., Wang, Z.P., Zhang, H.Y., Han, C.Y., Liu, B., Wang, X.C. *et al.* (2014) A CRISPR/Cas9 toolkit for multiplex genome editing in plants. *BMC Plant Biol.* **14**, 327.

Xu, M., Wang, X., Liu, J., Jia, A., Xu, C., Deng, X.W. and He, G. (2022) Natural variation in the transcription factor REPLUMLESS contributes to both disease resistance and plant growth in *Arabidopsis*. *Plant Commun.* **3**, 100351.

Yao, X., Li, H., Nie, J., Liu, H., Guo, Y., Lv, L., Yang, Z. *et al.* (2023) Disruption of the amino acid transporter CsAAP2 inhibits auxin-mediated root development in cucumber. *New Phytol.* **239**, 639–659.

Zhang, J., Li, W., Xiang, T., Liu, Z., Laluk, K., Ding, X., Zou, Y. *et al.* (2010) Receptor-like cytoplasmic kinases integrate signaling from multiple plant immune receptors and are targeted by a *Pseudomonas syringae* effector. *Cell Host Microbe*, **7**, 290–301.

Zhang, J., Shao, F., Li, Y., Cui, H., Chen, L., Li, H., Zou, Y. *et al.* (2007) A *Pseudomonas syringae* effector inactivates MAPKs to suppress PAMP-induced immunity in plants. *Cell Host Microbe*, **1**, 175–185.

Zhao, T., Rui, L., Li, J., Nishimura, M.T., Vogel, J.P., Liu, N., Liu, S. *et al.* (2015) A truncated NLR protein, TIR-NBS2, is required for activated defense responses in the *exo70B1* mutant. *PLoS Genet.* **11**, e1004945.

Zhou, Z., Bi, G. and Zhou, J.M. (2018) Luciferase complementation assay for protein-protein interactions in plants. *Curr. Protoc. Plant Biol.* **3**, 42–50.

Zipfel, C., Kunze, G., Chinchilla, D., Caniard, A., Jones, J.D., Boller, T. and Felix, G. (2006) Perception of the bacterial PAMP EF-Tu by the receptor EFR restricts Agrobacterium-mediated transformation. *Cell*, **125**, 749–760.

Zipfel, C., Robatzek, S., Navarro, L., Oakeley, E.J., Jones, J.D., Felix, G. and Boller, T. (2004) Bacterial disease resistance in *Arabidopsis* through flagellin perception. *Nature*, **428**, 764–767.

Zárský, V., Cvrcková, F., Potocký, M. and Hála, M. (2009) Exocytosis and cell polarity in plants – exocyst and recycling domains. *New Phytol.* **183**, 255–272.

Supporting information

Additional supporting information may be found online in the Supporting Information section at the end of the article.

Figure S1 Genotyping and phenotypic analysis of *Csexo70b* mutants.

Figure S2 CsExo70B interacts with CsERECTA and CsCLV1 in *N. benthamiana* plants.

Figure S3 Knockout of *CsERECTA* resulted in dwarfed plants, smaller male flowers and seeds in cucumber.

Figure S4 The bimolecular fluorescence complementation (BiFC) assays showing CsExo70B interacts with CsERECTA, CsFLS2 and CsLYK5.

Figure S5 Detection of the specificity of CsERECTA, CsLYK5 and CsH$^+$-ATPase antibodies.

Figure S6 KEGG enrichment analyses of common up-regulated DEGs in *Csexo70b-5*[#] and *Cserecta-2*[#] mutants.

Figure S7 KEGG enrichment analyses of common down-regulated DEGs in *Csexo70b-5*[#] and *Cserecta-2*[#] mutants.

Figure S8 Knockout of *CsExo70B* promotes *Fusarium oxysporum* f. sp. *Cucumerinum Owen* (*Foc*) infection in cucumber.

Figure S9 The expression level of *CsFLS2* was normal in *Csexo70b* mutants and *CsExo70B*-OE lines.

Figure S10 Phenotypic analysis of *CsExo70B* overexpression lines.

Figure S11 The phenotypes of *Csexo70b* mutants.

Figure S12 Heat map showing the expression pattern of genes involved in auxin-related and cell division-related pathway.

Figure S13 Expression patterns of *CsERECTA*, *CsFLS2* and *CsLYK5* in cucumber different tissues.

Figure S14 Pathogen-induced *RK* expression in cucumber.